Paper 171

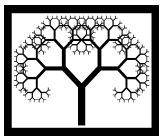

Proceedings of the Second International Conference on Railway Technology: Research, Development and Maintenance, J. Pombo, (Editor),
Civil-Comp Press, Stirlingshire, Scotland.

Wayside Measurement of Lateral and Vertical Wheel/Rail Forces for Rolling Stock Homologation

L. Bocciolini[1], A. Bracciali[2], L. Di Benedetto[1], R. Mastandrea[1] and F. Piccioli[2]
[1]Italcertifer SpA, Florence, Italy
[2]Department of Industrial Engineering (DIEF)
Università di Firenze, Florence, Italy

Abstract

International safety standards have set criteria to decrease the chances of railway vehicle derailment. The proneness of low-speed wheel flange climbing can be assessed in several ways; one of them includes a combination of measurements done on a twist test rig and on a track; the latter consisting of measuring lateral and vertical forces on a flat (non-canted) test track made of a 150 m curve radius without transition run, under high adhesion conditions.

This paper describes an advanced measuring system based on ER strain gauges mounted on the rails capable to measure both the aforementioned forces and to provide an estimation of the wheel/rail contact points for a wheelset. This novel feature takes into account lateral/vertical cross effects due to the actual contact point location allowing unprecedented accuracy and repeatability of these kind of measurements, that are not to be confused with existing weighing in motion (WIM) classical measurements.

Existing literature, FEM simulations, design of the calibration devices, calibration phase, tests on the measuring system and its delivery are described. Amongst the trains used to validate the functionality of the bench were an ultra-high speed train, a flat freight wagon, a locomotive and an EMU trainset, all with satisfactory results.

Keywords: railway, rolling stock, safety, derailment, testing, homologation, lateral forces, vertical forces.

1 Introduction

Safety against derailment is described in European Standard EN 14363:2005 [1]. One of the most critical situations that can be found in practice is the negotiation of sharp curves at low speed when a vehicle runs on twisted track with a high coefficient of friction. It is well known, in fact, that these conditions promote wheel flange climbing and low-speed derailments, which in fact occur normally within stations, marshalling yards and depots.

The European Standard, which descends from the report ERRI B55 Rp8 and the UIC 518 leaflet for the part regarding the safety against derailment, gives several possibilities to measure the attitude of a vehicle while running on twisted track. This check is mandatory for all new vehicles and is crucial especially for high speed trains where bogie-carbody connections are normally quite stiff (and damped) to limit hunting at the top operating speed, for vehicles with secondary pneumatic suspensions deflated due to the high torsional stiffness of the carbody, and for unloaded freight wagon due to low wheel loads and long wheelbase which increases the angle of attack of the front wheelset.

The measuring system described in this paper was developed and implemented in the frame of the collaboration between the University of Florence and Italcertifer S.p.A., a *Notified Body* and one of the Italian *Independent Safety Assessors*, which can also provide a large set of the measurements requested for the admission in service of a train in the laboratories located in Osmannoro, near Florence.

The system is made of several strain measuring points on both the rails of a 150 m-radius curve and is able to reconstruct with a high accuracy lateral/vertical forces and wheel/rail contact point for each wheel. As long as instrumented wheelsets are no longer needed for this test, this device can be used to check almost every kind of rolling stock with standard gauge, opening interesting scenarios also for the fast verification of "aggressiveness" of all existing vehicles.

2 Literature survey

Although the measurement of wheel-rail contact forces has a fundamental importance in railway safety and there is therefore plenty of scientific papers, they are in most cases of low or no use for the present research.

While weighing a vehicle in motion is a quite well developed field, accurate measurement of *both* lateral and vertical forces for service authorization of a vehicle are much more rare. Restricting the field to papers dealing with mutual wheel-rail interaction measurements and discarding those dealing with instrumented wheelsets, all of them indicate that electric resistance strain gauges (ER) attached to the rail are the most appropriate sensor to detect rail deformation from which loads may be inferred by proper calibration.

All the papers that have some relevance are quite old, do not consider the actual wheel-rail contact position and make low or no use of finite element models (FEM). As a matter of fact, in the last 30 years there were no real advances in this kind of measurements while, as it will be shown in this paper, improvements may be relevant. Rather than summarising here the results of the literature survey, for the sake of simplicity the most relevant approaches will be discussed in the following chapters.

3 Finite Element simulations

3.1 Introduction

Literature survey showed that the different measuring methods have complementary properties and that, for example, the actual wheel-rail contact position influences more one method than the others. That's why numerous configurations were analysed with linear elastic finite element simulations with the aim of finding information not only on the exchanged forces but also on contact point location.

In the following, after a description of strain gauge positioning, nominal sensitivities and the influence of the contact point are shown for each case. A paragraph will deal with cross-sensitivity (or cross-talk), the effect that generates the highest perplexity on the behaviour of the different measuring setups.

Through the use of a static FE model of a vertical (non inclined) 60E1 rail resting on elastic supports (fastenings, sleepers, ballast) with a sleeper spacing of 0.6 m it was possible to estimate all those factors that in the (quite old) literature were either neglected or seen as inevitable "side effects". The most important innovation of the present work is the investigation of a simultaneous application of a number of methods that is higher than that strictly needed as long as not only lateral and vertical forces but also the contact point position is of interest.

FE model was set by using ANSYS 13.0 Workbench, simulating 8850 mm of rail with R=150 m. Some small surfaces were generated on the rail surface in order to apply loads as the solver does not allow to impose forces directly on nodes. More than 330.000 SOLID187 elements were used with 20 mm size, except for the area where the results will be evaluated where element size was decreased to 5 mm.

The rail is resting on 14 supports spaced by 600 mm whose vertical stiffness (=51.8 kN/mm) simulates the combined stiffness of railpad and ballast. Lateral stiffness, calculated similarly, is 48.9 kN/mm. These values descend from literature values of 150 kN/mm and 280 kN/mm for vertical and lateral stiffness of rail fastenings and of 80 kN/mm and 60 kN/mm vertical and lateral stiffness of ballast ("per sleeper end"). The values found in the literature may vary considerably; the reader is referred to [2] for a survey of the values found from numerous references.

An iterative procedure, described later, allows to numerically reconstruct with a very good reliability the contact point location giving a definitely better estimation of the contact forces mutually exchanged.

Once again it is worth to underline that all these considerations, that are never present in the available literature, are needed as long as the development of a measuring equipment for certification of new vehicle is discussed here. Clearly the requirements of existing Y/Q measuring equipment and, even more, of WIM system are much less stringent leading to the intrinsically lower accuracy of those methods.

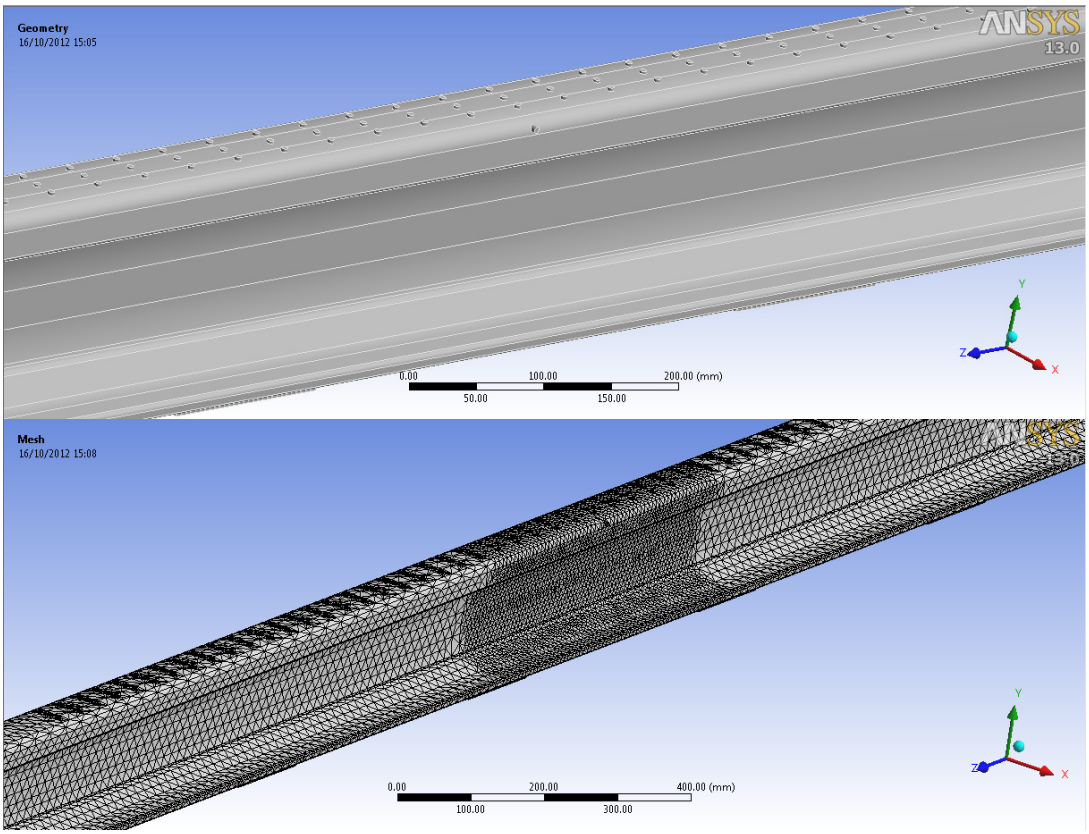

Figure 1: Geometry of the FE model. Small surfaces created for load applications can be seen.

Existing strain gauges layouts are considered and compared here for different reasons. It should be preliminary noted that the measurement of vertical forces Q is well known and documented; the corresponding layout can almost completely reject the effects of a lateral force Y which generates shear, bending in the horizontal plane and torsion. On the contrary, it is not easy to find a strain gauge layout that efficiently rejects the effects of Q and, what's more important, shear, horizontal bending and torsion due to Y. Three available methods were analysed which intrinsically provide different results; these differences become a fundamental input for the contact point determination that will be described hereinafter. The discrepancies between the numerical model and the track where tests were made and their influence on the quality of the measurements will be described as well.

3.2 Estimation of the vertical force Q (bridge S_Q)

All the literature agrees on the fact that the best system to measure the vertical force consists of two sets of strain gauges on the rail web installed at 45° (*chevron* configuration) symmetrically with respect to the sleeper bay centre. This layout measures the difference of shear between the two sections and results therefore insensitive to the actual position of the vertical load as long as it is included between the sections. This results in a (theoretically) constant measured value for several dozen centimetres making the measurement more robust.

The configuration consists of 8 strain gauges in a full Wheatstone bridge where the signal of all ER sums up for vertical forces and cancels for lateral forces. Quite recently, the Italian infrastructure manager RFI has emitted a technical specification for the supply of measuring systems of this kind [3] that are nevertheless widespread since many years in other countries.

3.3 Three methods to estimate the lateral force *Y*

The first of the three methods found in the literature for the measurement of the effects of lateral forces is described in [4], which descends from UIC/ORE studies ("*French method*" from now on). The method consists in measuring the strains due to bending moment in the horizontal plane generated by a lateral force *Y* by means of ER strain gauges vertically mounted on the rail web, symmetrically respect to the horizontal neutral plane. As the shear force is by definition the variation of bending moments evaluated on two distinct sections, the method allows to estimate the lateral shear force in a give section as

$$T = \Delta M / \Delta y \tag{1}$$

Bending moments are inevitably affected by rail boundary conditions (according to rail and support stiffness). ORE studies found that an estimation of lateral forces with this method is possible but, as bending moments vary continuously, will give a changing value depending on all mentioned parameters (distance of instrumented sections, rail stiffness, support stiffness). The layout was therefore simulated varying these parameters. The final layout, optimised for a 60E1 rail with sleeper spacing of 60 cm, is shown in Figure 2. A full Wheatstone bridge is used with 8 ER strain gauges.

The second method is described by Ahlbeck and Harrison ([5],[6],[7]) that first proposed a measuring layout based on the use of strain gauges installed on the rail foot in the *chevron* configuration ("*American method*" from now on). This method has several analogies with the one for the measurement of vertical forces as long as it estimates the lateral force by the difference of shear forces measured directly (and not estimated as in the French method). Also in this case a full Wheatstone bridge is used with 8 ER strain gauges.

The third method is the oldest one (again cited by Ahlbeck and Harrison) and although it was then abandoned, it is nevertheless interesting for a feature that will be described later. The method is similar to the French one, but strain gauges are mounted in correspondence of the axis of a sleeper in order to give the maximum stiffness to lateral loads and therefore the maximum bending of the rail web ("*on-sleeper method*" from now on). Several reasons led to discard this method: it gives only local estimations of *Y* that must be identified from a single peak and proved to be very sensitive to the effect given by the lateral position of *Q*. This sensitivity will be used there to evaluate the actual position of the contact point. In this case a full Wheatstone bridge with 4 ER strain gauges is used.

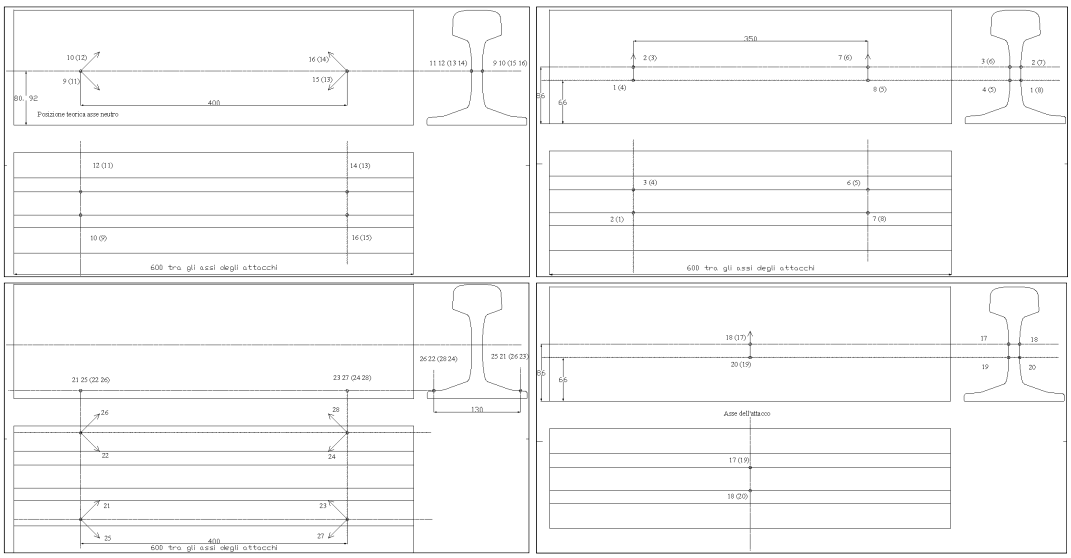

Figure 2: Strain gauges position for *Q* estimation (top left), *Y* estimation with the *French method* (top right), *Y* estimation with the *American method* (bottom left) and *Y* estimation with the *on-sleeper method* (bottom right).

3.4 Optimal separation of instrumented sections and nominal sensitivity of measuring bridges

A set of static FE simulations was conducted by separating the sections for the measurement of lateral forces *Y* by 200 mm, 300 mm, 350 mm and 400 mm. This allowed to check the shape and the regularity of the signals reducing the possible errors during measurements.

The following was observed (Figure 3):

- the signal S_y from the *French method* changes from one maximum to two local maxima, resulting "very flat" for the 350 mm separation and it is not affected by the force applied more than 2 m away from the centre of the section;
- the signal S_{yh} from the *American method* has only one maximum regardless of the separation of sections, with different "peakedness" and an amplitude that grows with the separation, having moreover an influence longer than 1.5 m from the centre;
- the signal S_{yt} from the *on-sleeper method* is intermediate between the previous, with a distance of influence in between the French and the American method and with a lower sensitivity.

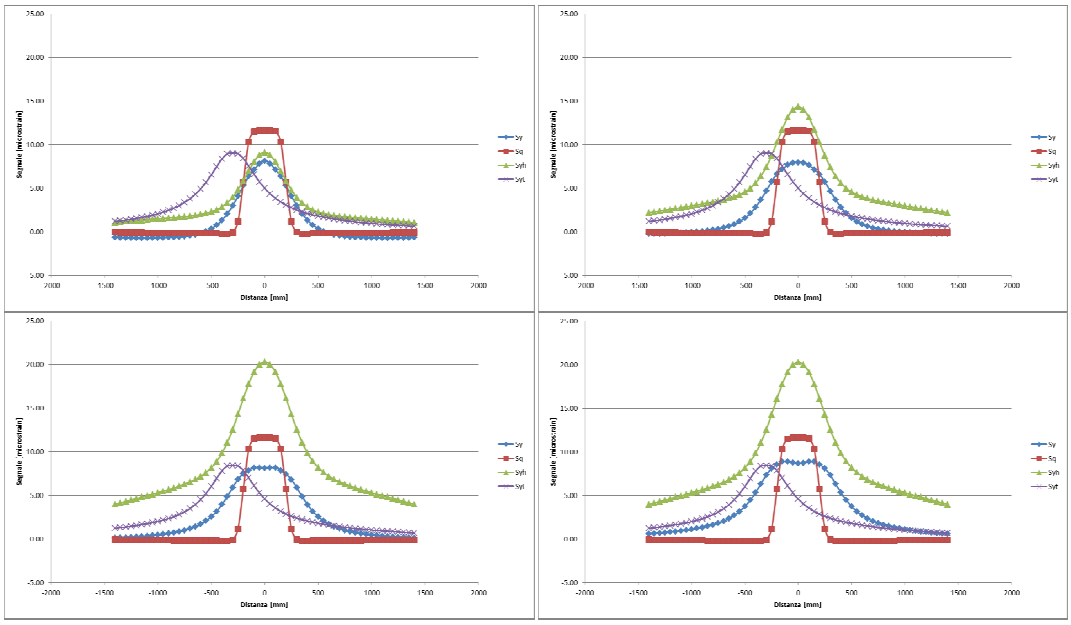

Figure 3: Left to right, top to bottom: strains from lateral force Y with French bridge (blue), American bridge (green) and on-sleeper bridge (magenta) for 200 mm, 300 mm, 350 mm and 400 mm separation. Also results for vertical bridge with constant separation of ER bridges (400 mm) are shown in red.

For this reason the final spacing used for simulation was 350 mm resulting in the sensitivity of the various bridges. Under the hypothesis of linearity, the general relationship between the measured signal S [με] and the applied force F [kN] will be given by the equation

$$S = K\,F \tag{2}$$

where K is the sensitivity in με/kN. When the load is either purely vertical or purely lateral and applied on the centre point of the rail crown the sensitivity is defined "nominal". For the vertical, the French and the American methods Q is applied at the midspan, resulting in K_q, K_6 and K_4 nominal sensitivities; for the on-sleeper method Q is applied over the sleeper, resulting in K_2 nominal sensitivity. The values found from the simulations are shown in Table 1. It can be seen that all the measuring layouts result in quite high strain levels on the rails, allowing measurements of good quality, favoured by the fact that only temperature-compensated full Wheatstone bridges are going to be used.

Nominal sensitivity	Value
On-sleeper method K_2	8.12 με/kN
American method K_4	-20.15 με/kN
French method K_6	-8.13 με/kN
Vertical K_Q	-11.74 με/kN

Table 1: Values of nominal sensitivities

4 Influence of the wheel-rail contact point position (CPP)

Wheelsets do not normally run centred when negotiating a curve. The front wheelset of a bogie typically runs with the external wheel flange in contact with the rail shoulder, while the rear wheelset may run displaced to the left or to the right depending on many parameters whose description lies outside the scope of this paper.

As long as wheels and rails have specific profiles that couple in a peculiar way, it is important to evaluate the influence of the point of application of the mutual forces between the wheel and the rail. This point will be called "contact point position" (CPP) and the forces will be considered applied to this point and not to the contact patch resulting from bodies elasticity. This is not a limit since the total force is responsible of the effects that are shown hereinafter.

Shifting laterally the contact point leads also to the variation of its height when the displacement reaches the extreme values (for the 60E1 rail coupled to the ORE S1002 profile this happens when the wheelset is displaced by 37 mm on a standard gauge track), changing the torsion component given by the lateral force (Figure 4).

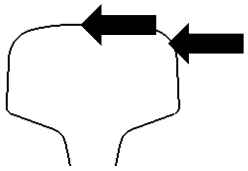

Figure 4: Change of the contact point height for the largest lateral displacements of a wheelset.

By changing the lateral CPP from +15 mm (outwards) to -40 mm (inwards) under the application of a pure Q, a difference lower than 0.01 με/kN in the nominal sensitivity of the vertical bridge shown above of -11.74 με/kN was observed. This confirms that the method for the measurement of vertical forces is insensitive to CPP. The *French method* shows a little dependency from the CPP where a lateral force Y is applied, while a larger sensitivity affects the *on-sleeper method* and even more the *American method* (see Table 2 and Figure 5)

Method considered	Contact point position					Max variation
Sensitivity in με/kN	15 mm	0 mm	-15 mm	-37 mm	-40 mm	
French K_6	-8.13	**-8.13**	-8.13	-8.03	-8.04	-1.23 %
American K_4	-20.14	**-20.15**	-20.14	-18.44	-18.42	-8.59 %
On-sleeper K_2	8.12	**8.12**	8.12	8.53	8.51	+4.69 %

Table 2: Change in sensitivity due to lateral CPP

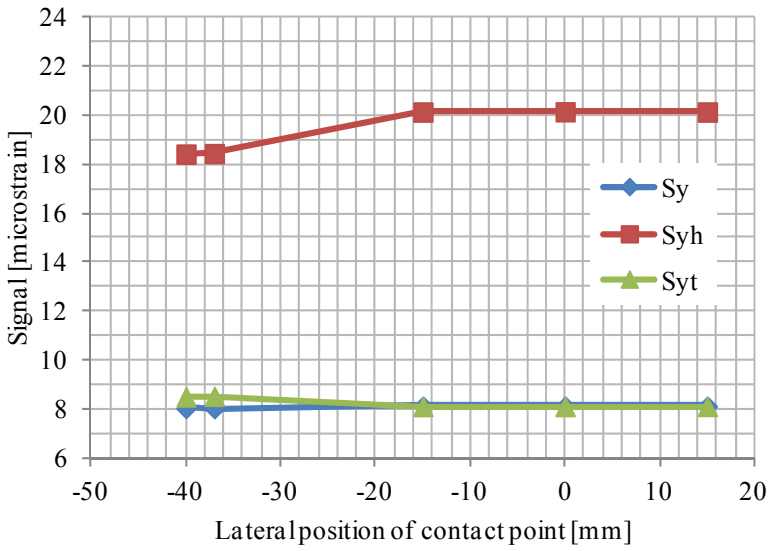

Figure 5: Influence of the CPP of a vertical load on the response of lateral force measuring bridges (note: absolute values taken for better visualization).

It is important to highlight that the maximum differences appear for the largest lateral displacements (-37 mm and -40 mm) and are due to the change in the height of the CPP which follows the railhead profile. As long as this change influences only the bending moment to which all of methods for lateral force estimation are sensitive, in the following the sensitivities K_2, K_4 and K_6 will be considered linearly changing with the height of the CPP.

5 Cross-sensitivity (cross-talk)

Theoretically Q should give an output only on the corresponding bridge with sensitivity K_Q, while Y should affect only the corresponding sensitivities K_2, K_4 and K_6. This will not be in practice the case at least for shifted CPP, but in the following this will be verified also for the centred case. This check is fundamental because while a pure Q can theoretically exist, a Y will always be coupled with Q. As long as the Y/Q ratio can reach values close to 1, numerical tests with Q=Y=1 kN will be considered as well as the nominal cases with Q=1 kN and Y=1 kN.

5.1 Cross-talk with nominal (centred) *Q* and *Y* forces

Table 3 shows the sensitivities resulting from the application of Q, Y and Y+Q on all the bridges. It can be seen that the cross-influence is negligible, being always lower than 1%.

	Applied forces		
	Q=1 kN	Y=1 KN	Q=Y=1 kN
Vertical method K_Q [με]	**K_Q=-11.74**	-0.04	-11.64 (-0.8%)
French method K_6 [με]	-0.04	**K_6=-8.13**	-8.16 (+0.4%)
American method K_4 [με]	-0.08	**K_4=-20.15**	-20.19 (+0.2%)
On-sleeper method K_2 [με]	0.01	**K_2=8.12**	8.13 (+0.1%)

Table 3: Cross-talk with nominal forces

5.2 Influence on the estimation of *Y* due to a lateral shift of *Q*

Lateral shift of *Q* introduces a torsion that, although not influencing the estimation of *Q*, influences the estimation of *Y*. As long as the torsion is directly proportional to the lateral shift, the effect was evaluated for a limited number of points confirming the linearity of this effect (Figure 6).

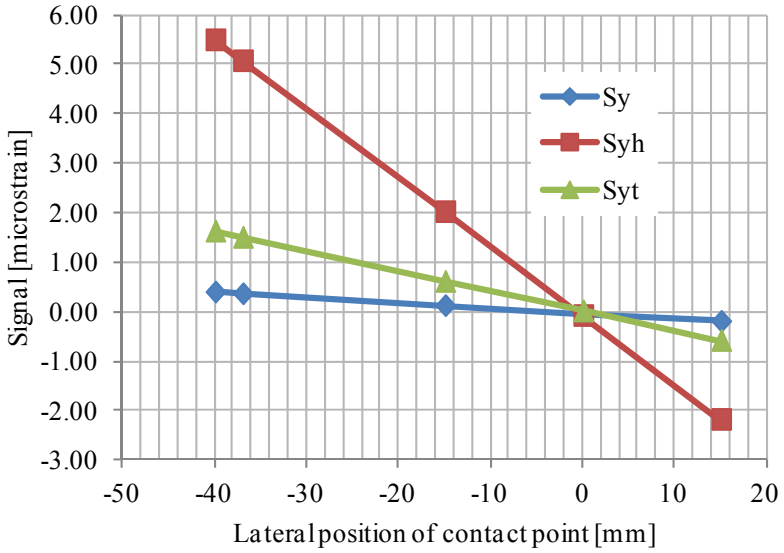

Figure 6: Influence on estimation of *Y* due to *Q* shift for the three methods considered.

Considering for example a quite standard shift (-15 mm, CPP that can be easily reached during the transit in the 150 m-radius curve), the following cross sensitivities were found:

- *French method* (K_6=-8.13 με/kN): 0.12/(-8.13) = -1.5 %
- *American method* (K_4= -20.15 με/kN): 2.02/(-20.15) = -10.0%
- *On-sleeper method* (K_6= 8.12 με/kN): 0.61/8.12 = +7.5 %

For example a Q=100 kN (10 t) laterally shifted by 15 mm produces a signal on the *American method* bridge close to -10 kN (-1 t), an error that is certainly not acceptable. The following equations were therefore used to relate the signal of the bridges for Y estimation as a function of the lateral displacement of Q with the introduction of the corresponding constants K_5, K_3 and K_1:

$$\begin{aligned} &\textit{French method}: && \Delta S_y = && K_5\, Q\, x = -0.0108\, Q\, x \\ &\textit{American method}: && \Delta S_{yh} = && K_3\, Q\, x = -0.1394\, Q\, x \\ &\textit{On-sleeper method}: && \Delta S_{yt} = && K_1\, Q\, x = -0.0402\, Q\, x \end{aligned} \qquad (3)$$

5.3 Influence on the estimation of *Y* due to a lateral shift of *Q* and *Y*

While a purely vertical shifted force Q is conceivable, a purely lateral force Y acting on the rail doesn't exist. That's why the combined presence of Q and Y moving simultaneously along the railhead crown profile was considered. It was confirmed that the estimation of Q is unaffected; the effects on the bridges for the estimation of the lateral force Y can be seen in Figure 7.

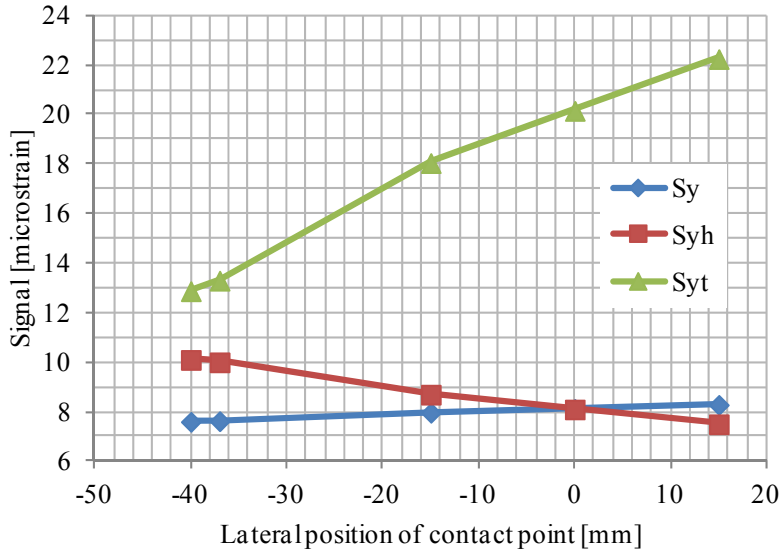

Figure 7: Influence on estimation of Y due to Q shift for the three methods considered (note: absolute values taken for better visualization).

Beyond the effect of the torsion given by the vertical component, the change in the estimation derives from the shift of the vertical location of the CPP which affects the various bridges. No equations are derived as the effect of this cause will be automatically considered in the iterative procedure that will be described later; it is only supposed that the changes introduced by the variation of the z-coordinate of the CPP are proportional to its value, as confirmed by the simulations shown.

6 Estimation of the lateral force *Y* and of the CPP

6.1 Introduction

It was shown that the lateral displacement of the CPP results in a non-negligible variation of the reading of the ER bridges. In particular, while the vertical force is always correctly estimated, the estimation of lateral forces is linearly influenced by the lateral displacement of CPP, resulting in a cross-talk that can be properly taken into account only by estimating also the current CPP.

It is not therefore in general sufficient to measure any of the three pairs S_Q - S_y, S_Q - S_{yh}, or S_Q - S_{yt}, to get the desired values of Q and Y as measured values are correlated. The availability of three linearly independent measuring methods allows to write the following three systems of equations:

$$\begin{cases} S_Q=K_Q\cdot Q \\ S_{yt}=K_1\cdot Q\cdot x+K_2\cdot Y \\ S_{yh}=K_3\cdot Q\cdot x+K_4\cdot Y \end{cases} \quad \begin{cases} S_Q=K_Q\cdot Q \\ S_{yt}=K_1\cdot Q\cdot x+K_2\cdot Y \\ S_y=K_5\cdot Q\cdot x+K_6\cdot Y \end{cases} \quad \begin{cases} S_Q=K_Q\cdot Q \\ S_{yh}=K_3\cdot Q\cdot x+K_4\cdot Y \\ S_y=K_5\cdot Q\cdot x+K_6\cdot Y \end{cases} \tag{4}$$

These equations are based on the following hypotheses:

- S_Q depends only on the value of the vertical force Q;
- S_{yh}, S_y and S_{yt} depend on the value of the vertical force Y and on the torsion $Q\cdot x$;
- the force Y does not change from the sleeper to the midspan.

The system of equations can be expressed as follows:

$$\begin{cases} Q=\dfrac{S_Q}{K_Q} \\ x=\dfrac{\left(\dfrac{S_{yt}}{K_1\cdot Q}-\dfrac{K_2\cdot S_{yh}}{K_3\cdot K_1\cdot Q}\right)}{\left(1-\dfrac{K_2\cdot K_3}{K_1\cdot K_4}\right)} \\ Y=\dfrac{S_{yh}-K_3\cdot Q\cdot x}{K_4} \end{cases} \quad \begin{cases} Q=\dfrac{S_Q}{K_Q} \\ x=\dfrac{\left(\dfrac{S_{yt}}{K_1\cdot Q}-\dfrac{K_2\cdot S_y}{K_5\cdot K_1\cdot Q}\right)}{\left(1-\dfrac{K_2\cdot K_5}{K_1\cdot K_6}\right)} \\ Y=\dfrac{S_y-K_5\cdot Q\cdot x}{K_6} \end{cases} \quad \begin{cases} Q=\dfrac{S_Q}{K_Q} \\ x=\dfrac{\left(\dfrac{S_{yh}}{K_3\cdot Q}-\dfrac{K_4\cdot S_y}{K_5\cdot K_3\cdot Q}\right)}{\left(1-\dfrac{K_4\cdot K_5}{K_1\cdot K_6}\right)} \\ Y=\dfrac{S_y-K_5\cdot Q\cdot x}{K_6} \end{cases} \tag{5}$$

6.2 Iterative solution of the system of equations

While the value of Q is estimated directly for the first equation, the remaining two cannot be solved directly as the value of the parameters K_2, K_4 and K_6 are a function of the height z of the actual CPP.

A simple iterative procedure was therefore set up, starting from the measured (simulated) values of the outputs of the bridges S_y, S_{yh} and S_{yt} depending on the selected combination of measuring systems. Supposing, for example, to choose the *French method* (K_6) and the *American method* (K_4), i.e. the last of the three systems (5), the iterative procedure is as follows:

1. a first value of the eccentricity x_0 is calculated from the second equation;
2. a corresponding value of the estimated lateral force Y_0 is calculated from the third equation;
3. by using the description of the railhead profile, a corresponding height z_0 is calculated;
4. the corrected values of the parameters $K_4(z_0)$ and $K_6(z_0)$ are calculated;
5. the actual values of x_i and Y_i are calculated;
6. the actual value of z_i is calculated;
7. the actual values of $K_4(z_i)$ and $K_6(z_i)$ are calculated;
8. $i=i+1$ and the process is iterated from 5 step until $|(Y_i-Y_{i-1})/Y_{i-1}| < 0.01$

The algorithm was validated through a set of cases where different combinations of forces were applied to the FEM model in predefined positions. The intention was to check the ability of the proposed system to reconstruct both the magnitude of the forces and the CPP by using the parameters and the iterative procedure described.

Results are shown in Table 4. It can be seen that from a numerical point of view the CPP estimation is similar with the three possible pairs. Cases 7, 8 and 9 consist of two Q and Y forces applied at x=0 mm and x= -37 mm, simulating a "double contact" position, i.e. the simultaneous contact of the wheel tread *and* of the wheel flange on the railhead. All pairs find an "equivalent" lateral position that satisfies the criterion of convergence although the solutions clearly has no physical meaning.

7 System implementation and calibration

The application of lateral calibration loads is trivial, consisting in a hydraulic jack interfaced with a load cell and a proper device which allows to give arbitrary force at some different predefined heights. This was clearly needed to evaluate the influence of the z level of the contact point position.

The application of calibration vertical loads was obtained by means of a standard freight wagon series H to which a laterally adjustable device was applied consisting of a hydraulic jack and a load cell. The advantage of this solution is that through the use of a slider driven by a screw allows a continuous and arbitrary lateral positioning of the vertical forces. Also in this case some predefined positions were available to calibrate the system considering the torsion given by a displaced application of the vertical load. Both the systems are shown in Figure 8.

Case	Applied forces and lateral displacement of CPP	French + On-sleeper	American + On-sleeper	French + American
1	*Q*= 1 kN *Y*= 0 kN *x*= 0 mm	1.000 kN 0.004 kN 0.587 mm	1.000 kN 0.002 kN 0.231 mm	1.000 kN 0.005 kN -0.170 mm
2	*Q*= 1 kN *Y*= 0 *x*= - 37 mm	1.000 kN -0.004 KN -36.432 mm	1.000 kN 0.003 kN -36.733 mm	1.000 kN 0.005 kN -37.027 mm
3	*Q*= 1 kN *Y*= 1 kN *x*= 0 mm	0.992 kN 1.003 kN 0.395 mm	0.992 kN 1.002 kN 0.064 mm	0.992 kN 1.004 kN -0.308 mm
4	*Q*= 1 kN *Y*= 1 kN *x*= - 15 mm	0.991 kN 1.003 kN -14.194 mm	0.991 kN 1.001 kN -14.645 mm	0.991 kN 1.004 kN -15.218 mm
5	*Q*= 1 kN *Y*= 1 kN *x*= + 15 mm	0.992 kN 1.003 kN 15.099 mm	0.992 kN 1.002 kN 14.773 mm	0.992 kN 1.004 kN 14.405 mm
6	*Q*= 1 kN *Y*= 1 kN *x*= -37 mm	0.990 kN 1.003 kN -37.650 mm	0.990 kN 1.004 kN -37.516 mm	0.990 kN 1.003 kN -37.384 mm
7	*Q*= 0.5 kN + 0.5 kN *Y*= 0.2 kN + 0.8 kN *x*=0 mm - 37 mm	0.992 kN 1.005 kN -24.671 mm	0.992 kN 0.999 kN -25.593 mm	0.992 kN 1.008 kN -26.010 mm
8	*Q*= 0.2 kN + 0.8 kN *Y*= 0.2 kN + 0.8 kN *x*=0 mm - 37 mm	0.992 kN 1.004 kN -27.888 mm	0.992 kN 1.005 kN -27.595 mm	0.992 kN 1.003 kN -27.310 mm
9	*Q*= 0.2 kN + 0.8 kN *Y*= -0.2 kN + 1.2 kN *x*=0 mm - 37 mm	0.992 kN 1.004 kN -32.036 mm	0.992 kN 1.003 kN -32.264 mm	0.992 kN 1.005 kN -32.486 mm

Table 4: Lateral/vertical forces and contact point position estimated by the relative combination of measuring systems compared to known inputs

A preliminary set of tests was conducted by installing all the 4 systems shown in this paper (Figure 9), although for the final selection the combination of the *American method* and of the *French method* was preferred, as the on-sleeper method is quite sensitive to local fastening stiffness and results in a local estimation which is furthermore displaced with respect to the other bridges. The final system, consisting of an industrial 4 all-weather instrumented sections is shown in Figure 10.

The calibration was done by using the tools described for all the instrumented sections, resulting in the calibration constants shown in Table 5.

Figure 8: Devices for lateral and vertical test loads application and interface with the rail.

Figure 9: Left: application of ER strain gauges for Q and Y estimation. All the three methods for Y estimation are visible. Right: calibration under Q force.

Figure 10: Complete measuring system available at Firenze Osmannoro Italcertifer laboratories.

		Value of calibration constants [μV/V/kN]			Value of calibration constants [μV/V/kN/mm]	
Section	Side	Calibration of vertical forces K'_Q	Calibration of lateral forces with French method K'_6	Calibration of lateral forces with American method K'_4	Calibration of lateral forces with French method K'_5	Calibration of lateral forces with American method K'_3
1	right	2.79	1.60	6.23	$2.21 \cdot 10^{-3}$	$23.5 \cdot 10^{-3}$
	left	2.77	1.70	6.04	$1.41 \cdot 10^{-3}$	$25.8 \cdot 10^{-3}$
2	right	2.67	1.67	6.77	$4.17 \cdot 10^{-3}$	$32.1 \cdot 10^{-3}$
	left	2.79	1.67	6.33	$3.16 \cdot 10^{-3}$	$38.7 \cdot 10^{-3}$
3	right	2.72	1.64	7.67	$1.06 \cdot 10^{-3}$	$25.9 \cdot 10^{-3}$
	left	2.72	1.51	7.03	$0.85 \cdot 10^{-3}$	$20.3 \cdot 10^{-3}$
4	right	2.71	1.57	6.62	$1.38 \cdot 10^{-3}$	$21.8 \cdot 10^{-3}$
	left	2.77	1.64	6.37	$1.78 \cdot 10^{-3}$	$11.2 \cdot 10^{-3}$

Table 5: Experimentally determined values of calibration constants

As long as the outputs from FE calculations were expressed in με while the readout of the measuring system is clearly in Volts, the fundamental equation of strain gauge full bridges applies:

$$\frac{\Delta V}{V} = \frac{K}{8}\Delta\varepsilon$$

where $\Delta V/V$ is the output with reference to supply voltage and $\Delta\varepsilon$ is the signal expressed in με. Since the strain gauge constant $K \cong 2$, this leads to the following formula:

$$\frac{\Delta V}{V} = \frac{1}{4}\Delta\varepsilon$$

This allows for a direct comparison of the estimated and the measured calibration values, as shown in Table 6, where a good agreement is visible for vertical forces while a lower agreement exists for lateral forces, with a higher sensitivity for the *American method* and a lower sensitivity for the *French method*. In all cases the standard deviation results good, meaning that the measuring system is reproducible in other sites with a high confidence on the outputs.

Calibration constant	K_Q [μV/V/kN]	K_6 [μV/V/kN]	K_4 [μV/V/kN]	K_5 [μV/V/kN/mm]	K_3 [μV/V/kN/mm]
Experimental values	2.74 ± 0.045	1.63 ± 0.062	6.63 ± 0.52	$2.00 \cdot 10^{-3}$ ± $1.14 \cdot 10^{-3}$	$24.9 \cdot 10^{-3}$ ± $8.15 \cdot 10^{-3}$
FEM Simulated values	2.93	2.03	5.04	$2.70 \cdot 10^{-3}$	$3.485 \cdot 10^{-3}$
Experimental/numerical difference	-6.6 %	-20 %	+32 %	-26 %	-28 %

Table 6: Comparison of calibration constants obtained from finite elements and from the experimental calibration procedure. Average and standard deviation values for the 4 instrumented sections are shown.

Differences in the order of 30% can be explained with the intrinsic limitations of the FEM simulation:

- sleeper spacing resulted in the field much higher (in the order of 700 mm) compared to the simulated value (600 mm);
- strain gauge positions were slightly varied to ease the installation procedure;
- track gauge was 1465 mm instead of 1435 mm, and this widening limited the use of the calibration devices that were designed for standard gauge.

Although these conditions were theoretically usable to update/refine the FE model and the calibration device, the results from the calibration phase were so satisfactory that it was decided to stop any further activity to immediately deliver the operating system to the laboratory.

8 Sample results

In this chapter the results obtained for a high speed EMU are shown. This vehicle is interesting as it is equipped with air springs as the secondary suspension, and both inflated and deflated conditions were tested and led to quite different results.

Vertical loads acting on each wheelset can be compared directly to the value measured on a precision balance as load change is almost negligible for a non-canted (flat) track. The results for the first axle are shown as an example in Table 7; it can be seen that the measuring station gives the values measured on the weighing machine with a maximum error of +2.56%, which is considered to be a very good result. This value is the maximum obtained also considering all the other wheelsets of the train under test (see Table 8)

Car	Direction	Measured Q [kN]	Axleload [kN]	Error %	Measured Q [kN]	Axleload [kN]	Error %
		Efficient (inflated) airspring			Inefficient (deflated) airspring		
1	Entering the curve with the first bogie	150.04	149.52	+ 0.35	152.19	149.52	+ 1.79
2		130.00	131.36	- 1.12	132.32	131.36	+ 0.73
3		121.88	121.24	+ 0.72	124.35	121.24	+ 2.56
1	All vehicles already in the curve	150.69	149.52	+ 0.78	151.70	149.52	+ 1.46
2		130.73	131.36	- 0.57	131.84	131.36	+ 0.37
3		123.10	121.24	+ 1.74	123.78	121.24	+ 2.09

Table 7: Measured and comparison axleloads for the first wheelset of each car

	Maximum error	Average Error
Inefficient (deflated) airspring	2.56 %	1.29 % ± 0.78 %
Efficient (inflated) airspring	2.41 %	1.16 % ± 0.66 %
All conditions	2.56 %	1.22 % ± 0.72 %

Table 8: Summary of the error on all axles

More complex considerations can be done on Y values. First of all the comparison with a different and better measurement does not exist; second the friction coefficient, defined as in [1], varies according to local conditions that change in time and make this measurement more variable by definition.

In any case it is possible to make consistency considerations with expected values obtained from similar previous cases or from experience. Table 9 describes 4 runs, one per combination of inflated or deflated airspring running in both directions. It is possible to find several evidences that show a good repeatability:

- considering that the listed axles are the first for each vehicle, all the vehicles have a similar behaviour when entering the curve with the first axle. Car 1 always gives the highest forces (with one exception) while cars 2 and 3 show a behaviour that changes according to the running direction;

- within a test type, the trend of the external Y force is coherent with the trend of the conventional friction coefficient (i.e. the Y/Q ratio on the inner rail);
- the force on the inner rail is always lower than that on the outer rail.

			Efficient (inflated) airspring			Inefficient (deflated) airspring		
	Pass-by #	Car	Y_{est} [kN]	$Y_{int.}$ [kN]	$Y/Q_{int.}$ [-]	$Y_{est.}$ [kN]	$Y_{int.}$ [kN]	$Y/Q_{int.}$ [-]
Entering the curve with the first bogie	1	1	40.0	30.6	0.46	46.8	32.8	0.50
		2	41.4	24.7	0.44	46.2	27.1	0.49
		3	34.5	19.0	0.37	40.7	24.5	0.48
	2	1	49.3	33.9	0.52	44.6	30.5	0.47
		2	47.7	28.3	0.52	43.5	23.0	0.42
		3	42.1	24.3	0.48	39.4	22.5	0.44
	3	1	46.0	33.8	0.51	46.0	29.5	0.45
		2	43.8	27.9	0.50	43.3	21.2	0.39
		3	36.6	25.1	0.47	33.4	20.7	0.39
	4	1	43.8	35.6	0.53	47.6	35.0	0.53
		2	43.4	29.6	0.52	47.7	27.6	0.51
		3	38.4	28.9	0.54	43.7	26.4	0.51
All vehicles already in the curve	1	1	40.5	29.4	0.44	40.4	31.8	0.48
		2	36.0	26.4	0.46	34.8	29.0	0.49
		3	37.4	26.0	0.49	36.4	28.6	0.53
	2	1	41.6	28.6	0.44	38.4	30.7	0.46
		2	34.8	25.8	0.45	32.7	26.4	0.45
		3	34.7	24.5	0.46	36.5	28.4	0.53
	3	1	40.1	28.8	0.44	38.4	31.6	0.47
		2	33.0	22.9	0.40	33.1	28.3	0.48
		3	35.6	21.9	0.42	36.7	29.3	0.54
	4	1	39.9	29.6	0.45	38.6	31.2	0.47
		2	33.1	25.0	0.43	33.7	28.7	0.49
		3	34.9	23.4	0.44	36.2	29.1	0.54

Table 9: Estimation of lateral forces and of the Y/Q ratio for the first axle of the three cars with efficient and inefficient secondary suspension

Table 10 shows the average values of Y/Q measured during 4 runs according to [1] for the four testing conditions. All the results appear quite logical, since:

- ratios with inefficient (empty) airspring are higher than those with efficient (filled) airspring;

- ratios entering the curve with the first bogie are higher than those on when the vehicle is already all in the curve;
- the inversion in the behaviour of cars 2 and 3 according to the running direction is confirmed.

Car	Direction	*Y*/*Q* outer rail Efficient airspring	Y/Q outer rail Inefficient airspring
1	Entering the curve with the first bogie	0.80	0.91
2		0.93	1.04
3		0.86	0.95
1	All the vehicle already in the curve	0.73	0.80
2		0.76	0.86
3		0.82	0.94

Table 10: Average values of the *Y*/*Q* ratio on the outer wheel according to [1]

To see the influence of the proposed system on the measurements made by the single bridges, the results are shown in the following tables:

- Table 11: Estimated and measured values for efficient suspensions while entering the curve with the first bogie;
- Table 12: Estimated and measured values for efficient suspensions with all the vehicle in the curve;
- Table 13: Estimated and measured values for inefficient suspensions while entering the curve with the first bogie;
- Table 14: Estimated and measured values for inefficient suspensions with all the vehicle in the curve

From these tables, the following conclusions can be drawn:

- for the first section, the *Y* value on the outer rail estimated by the solution of the system of equations is always greater than that measured by the French method (with only one exception);
- for the other sections, this value is always greater than both the French and the American methods;
- the *Y* value on the inner rail estimated by the solution of the system of equations is, for most of the cases, lower than the French method and higher than the American method;
- this last condition brings to a similar trend of the coefficient of friction as the vertical load is correctly estimated.

The estimation of lateral forces *Y* appears to be repeatable and coherent with the different testing conditions. The comparison with values estimated directly by the *French method* and the *American method* gives a more conservative estimation of the outer force (greater, except for section 1) and an intermediate estimation of the coefficient of friction, greater in any case than that measured by the *French method*.

		Outer rail			Inner rail		
Car	Meas. section	Y [kN]	Y_{Frech} [kN]	$Y_{\text{Amer.}}$ [kN]	Y [kN]	Y_{French} [kN]	$Y_{\text{Amer.}}$ [kN]
1	1	45.94	45.85	47.37	32.49	29.87	35.64
	2	46.68	45.27	44.69	31.42	31.70	40.04
	3	48.12	43.77	44.67	35.71	34.79	40.52
	4	43.40	39.60	41.38	35.78	29.60	35.50
2	1	44.11	43.85	45.95	29.36	28.97	35.02
	2	44.32	40.71	40.22	24.82	25.89	30.01
	3	44.31	40.43	41.96	27.56	24.84	29.60
	4	42.60	39.81	41.64	29.86	24.87	30.48
3	1	39.62	38.44	42.79	30.44	28.62	34.22
	2	38.85	36.38	35.87	24.33	24.08	30.58
	3	35.39	30.72	30.26	22.01	18.12	21.27
	4	32.53	29.85	30.41	23.81	19.55	23.84

Table 11: Estimated and measured values for efficient suspensions while entering the curve with the first bogie

		Outer rail			Inner rail		
Car	Meas. section	Y [kN]	Y_{Frech} [kN]	$Y_{\text{Amer.}}$ [kN]	Y [kN]	Y_{French} [kN]	$Y_{\text{Amer.}}$ [kN]
1	1	42.99	40.28	44.28	31.61	29.60	35.63
	2	41.71	38.85	37.17	27.99	30.07	38.24
	3	43.26	40.77	40.29	26.34	27.88	29.14
	4	34.21	27.21	26.80	31.59	25.56	30.85
2	1	35.99	34.71	38.25	29.48	27.06	32.59
	2	37.39	32.47	31.85	25.59	26.42	34.11
	3	36.91	27.01	25.30	22.99	24.78	24.89
	4	33.90	30.94	32.17	27.42	23.31	20.45
3	1	37.09	37.97	41.13	29.15	28.44	34.60
	2	39.80	35.99	34.93	23.86	24.18	31.00
	3	38.57	31.85	31.11	25.34	23.58	25.35
	4	34.33	30.63	31.74	25.80	21.70	26.10

Table 12: Estimated and measured values for efficient suspensions with all the vehicle in the curve

		Outer rail			Inner rail		
Car	Meas. section	Y [kN]	Y_{Frech} [kN]	$Y_{\text{Amer.}}$ [kN]	Y [kN]	Y_{French} [kN]	$Y_{\text{Amer.}}$ [kN]
1	1	47.20	46.39	51.49	34.27	32.28	36.96
	2	46.93	46.02	42.03	27.61	27.88	34.91
	3	46.04	41.86	42.37	31.76	28.81	32.20
	4	38.17	37.22	37.67	28.53	24.00	28.69
2	1	44.25	43.13	47.35	26.19	24.74	29.51
	2	45.16	42.82	41.01	21.21	20.85	26.41
	3	43.85	39.81	40.80	21.49	18.26	18.44
	4	40.93	40.94	41.59	23.21	20.04	23.99
3	1	38.20	36.59	40.27	21.81	18.86	20.81
	2	42.68	40.76	39.10	21.44	21.83	27.83
	3	38.71	34.25	34.29	21.82	19.85	20.91
	4	37.84	37.93	39.33	24.81	21.16	25.82

Table 13: Estimated and measured values for inefficient suspensions while entering the curve with the first bogie

		Outer rail			Inner rail		
Car	Meas. section	Y [kN]	Y_{Frech} [kN]	$Y_{\text{Amer.}}$ [kN]	Y [kN]	Y_{French} [kN]	$Y_{\text{Amer.}}$ [kN]
1	1	36.37	35.46	38.29	31.45	30.34	36.39
	2	40.41	35.04	33.19	26.85	26.69	34.14
	3	38.09	33.73	32.63	30.12	26.29	26.12
	4	39.63	35.70	36.70	36.49	31.23	38.00
2	1	30.81	28.24	30.70	29.01	27.07	32.58
	2	35.34	30.58	29.34	25.46	25.39	32.87
	3	33.97	29.95	28.13	28.00	25.75	30.05
	4	34.50	30.40	30.85	32.51	26.30	32.39
3	1	34.53	33.29	36.62	30.65	29.64	36.04
	2	36.44	32.28	32.02	24.87	24.96	32.36
	3	37.71	33.90	33.83	29.49	27.88	32.46
	4	36.26	32.86	34.38	31.52	26.91	33.24

Table 14: Estimated and measured values for inefficient suspensions with all the vehicle in the curve

9 Conclusions

The system described in this paper, developed by Italcertifer SpA and the University of Florence, can measure with an unprecedented level of accuracy lateral and vertical forces exerted by a train passing at low speed on a flat (non canted) curve with R=150 m.

This achievement was obtained through a careful comparison of the literature, an extensive FE analysis of a track, the design of the ER strain gauge bridges, the design of calibration devices and the application of the calibration procedures until the system is fully calibrated and operational.

At the date of writing of this paper (15 November 2013), Italcertifer has already tested according to European Standard EN 14363:2005 several vehicles, including a high speed train, a double-deck passenger car, a DMU trainset, a freight wagon and some service vehicles.

In all cases satisfactory results were obtained showing how the use of the new measuring system can significantly improve the quality of this kind of measurements, resulting in values that are markedly different from conventional systems.

References

[1] EN 14363, "Railway applications - Testing for the acceptance of running characteristics of railway vehicles - Testing of running behaviour and stationary tests", CEN, Brussels, 2005

[2] US Department of Transportation, report DOT/FRA/ORD-0408, "Reducing the Adverse Effects of Wheel Impacts on Special Trackwork", 2004

[3] Rete Ferroviaria Italiana, Technical Specification "Sistema di misura dei carichi verticali dinamici dei rotabili", doc. RFI_TCAR_SF_AR_12_003_B, 2013.

[4] A. Moreau: "La verification de la sécurité contre le déraillement sur la voie spécialisée de Villeneuve-Saint-Georges", Révue Générale des Chemins de Fer, April 1987, 25-32.

[5] D. R. Ahlbeck, H.D. Harrison: "Technique for Measuring Wheel/Rail Forces with Trackside Instrumentation", ASME Winter Annual Meeting, Atlanta, Georgia, 1977, Rpt. # 77-WA/RT-9.

[6] D. R. Ahlbeck, H.D. Harrison: "Techniques for Measurement of Wheel-Rail Forces", The Shock and Vibration Digest, 12(10), 1980, 31-41, 1980.

[7] H.D. Harrison, D.R. Ahlbeck: "Development and evaluation of wayside wheel/rail load measurement techniques", Proceedings of the International Conference on Wheel/Rail Load and Displacement Measurement Techniques, 19-20 Jan 1981, p. 8-1 / 8-20.